Available online at www.sciencedirect.com
SCIENCE DIRECT®
Journal of Power Sources 141 (2005) 272–285
JOURNAL OF POWER SOURCES
www.elsevier.com/locate/jpowsour

A dynamic simulation tool for hydrogen fuel cell vehicles

R.M. Moore[a,*], K.H. Hauer[b], D. Friedman[c], J. Cunningham[c], P. Badrinarayanan[c], S. Ramaswamy[c], A. Eggert[c]

[a] *Hawaii Natural Energy Institute, School of Ocean and Earth Science and Technology, University of Hawaii, Hawaii, HI, USA*
[b] *xcellvision, Major-Hirst-Strasse 11, 38422 Wolfsburg, Germany*
[c] *University of California, CA, USA*

Received 4 May 2004; accepted 29 May 2004

Abstract

This paper describes a dynamic fuel cell vehicle simulation (FCVSim) tool for the load-following direct-hydrogen (DH) fuel cell vehicle. The emphasis is on simulation of the direct-hydrogen fuel cell system (FC System) within the vehicle simulation tool. This paper is focused on the subsystems that are specific to the load-following direct-hydrogen model. The four major subsystems discussed are the fuel cell stack, the air supply, the water and thermal management (WTM), and the hydrogen supply. The discussion provides the details of these subsystem simulations. The basic vehicle configuration has been previously outlined by Hauer [An Analysis Tool For Fuel Cell Vehicle Hardware and Software (Controls) with an Application to Fuel Economy Comparisons of Alternative System Designs, Dissertation, UC California, Davis, USA, 2001] and Hauer and Moore [Fuel Cells for Automotive Applications, Professional Engineering Publishing, 2003, pp. 157–177, ISBN 1860584233] and is only briefly reviewed in this paper.

Keywords: Fuel cell vehicle; Simulation; Direct-hydrogen system; Fuel cell

1. Introduction

A new dynamic fuel cell vehicle simulation tool (FCVSim), that is designed for the analysis and evaluation of fuel cell vehicle (FCV) design options, has been introduced and described (Hauer [1] and Hauer and Moore [2,4,5]). This new tool was introduced following a benchmarking of publicly available FCV simulation tools (Hauer and Moore [3]). The primary attributes of *FCVSim* are:

- Emphasis on fuel cell vehicles,
- Logical forward-looking causal structure,
- Incorporation of dynamics aspects,
- Modular topology, and
- Preparation for hardware-in-the-loop and rapid prototyping.

This general dynamic FCV simulation tool is suitable for both industry and educational users. It was implemented as part of a 5 year R&D project on FCV simulation and analysis, sponsored primarily by an industrial consortium of approximately 20 companies (see "Acknowledgments" section at end of paper for further details on project and consortium). It is expected that this new fuel cell vehicle model will be applied in:

- Academia and government (teaching, policy analysis),
- The vehicle industry (analysis of alternative vehicle concepts), and
- The component industry (product planning, technology comparisons).

Versions of the *FCVSim* tool have been implemented for both load-following and hybrid FCV configurations and design options using hydrogen, methanol and hydrocarbon fuels. A total of 13 different load-following and hybrid FCV configurations have been simulated and analyzed using *FCVSim* (Hauer and Moore [2]).

* Corresponding author. Tel.: +1 808 956 2329; fax: +1 808 956 2336.
E-mail address: rmmoore@hawaii.edu (R.M. Moore).

0378-7753/$ – see front matter © 2004 Elsevier B.V. All rights reserved.
doi:10.1016/j.jpowsour.2004.05.063

Following a brief discussion of the general *FCVSim* tool, and a brief overview and introduction to the direct-hydrogen version of the *FCVSim* tool (namely the *DH-FCVSim* tool), this paper is organized around the description of the specific subsystems that are unique to the direct-hydrogen (DH) fuel cell system (FC System) in the *DH-FCVSim* tool.

There are four major subsystems that are specific to the load-following DH model, *DH-FCVSim*. They are:

- Fuel cell stack,
- Air supply system,
- Water and thermal management system, and
- Hydrogen supply.

In the four main sections of this paper, each of these four major subsystems is described, components and controls are discussed, the specific simulation methodology is described, and the general results available from the *DH-FCVSim* tool are illustrated by examples.

2. Review of general FCV simulation tool, *FCVSim*

This section reviews the general *FCVSim* model for the fuel cell vehicle and its main components and component arrangements, i.e., the structure of the general *FCVSim* simulation tool. The model uses a "forward-looking" methodology. A brief discussion of the "forward" and "backward" looking methodology is available in the literature (Hauer [1]). This model description begins on the most upper level, the vehicle. This level illustrates how the driver block interacts with the Vehicle block and how the drive cycle is utilized in the model. The uppermost level of the fuel cell vehicle model consists of the main blocks "Drive Cycle", "Driver" and "Vehicle" (Fig. 1).

The "Drive Cycle" block describes the demanded driving profile by specifying the velocity versus time. Examples of the standard US and international drive cycles utilized in *FCVSim* are listed by Hauer and Moore [2].

The "Driver" block represents the driver properties and driver characteristics. The main task for this block is the comparison of the driving cycle with the vehicle velocity. In the case when the simulated vehicle velocity is below the vehicle velocity specified in the drive cycle, the driver sends an acceleration command to the Vehicle block. In the case when the simulated vehicle velocity is above the specified velocity, the driver sends a brake signal to the Vehicle block. In a real vehicle the acceleration signal and the brake signal represent the position of the acceleration pedal and brake pedal.

From a systems point of view, the driver can be viewed as a controller for the "Vehicle" system. The inputs to the vehicle are the acceleration and brake commands and the system output is the vehicle velocity. The only criterion the driver block must meet is to ensure that the vehicle follows the drive cycle as closely as possible. In this respect the "Driver" block has the same task as a driver on an emissions test, namely following a given drive cycle within a specified tolerance band.

The Vehicle block of Fig. 1 contains the four sub-blocks "Drive Train", "Vehicle Curb", "FC System" and "Vehicle Controls", as illustrated in Fig. 2.

As noted above, the inputs to the overall Vehicle block are the brake pedal position and the acceleration pedal position (vehicle control signals generated by the driver block in Fig. 1), and the output of this block is the resulting vehicle velocity.

These two vehicle control signals are then utilized within the Vehicle block. The acceleration pedal position feeds into the Drive Train block and determines the fraction of the maximum motor torque that is supplied to the vehicle wheels. The brake pedal position feeds into the Vehicle Controls block. This block separates regenerative braking (in hybrid vehicles only) and mechanical braking. The request for regenerative braking is applied internally within the Drive Train block and controls the torque applied to the Vehicle Curb block, whereas the request for mechanical braking is fed directly to the Vehicle Curb block controlling the use of the mechanical brake system.

The Drive Train block includes models for the power electronics for the electric motor, the electric motor, and controls for the electric motor and the transmission. Depending on the driver request, expressed by the acceleration pedal position and brake pedal position, the Drive Train block provides torque to the wheels and draws current from the FC System block.

The Vehicle Curb block models the mechanical properties of the vehicle curb such as aerodynamic drag, rolling resistance, mass, etc. The inputs into this block are the applied wheel torque and the signal for the mechanical brake fraction. The outputs are the resulting vehicle velocity and the motor speed. In designs not considering tire slip, and us-

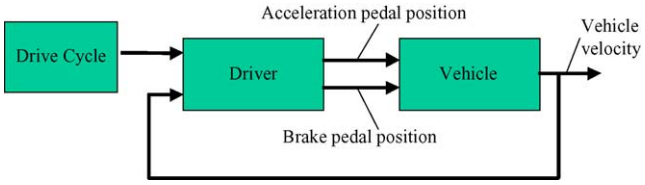

Fig. 1. Uppermost level of the general *FCVSim* model.

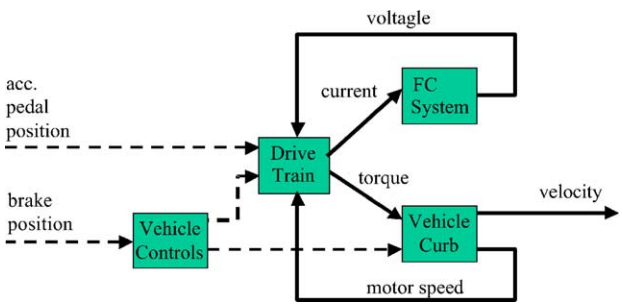

Fig. 2. Subsystems in Vehicle block.

ing a one-speed transmission, these two values are directly correlated.

The FC System block includes models for a fuel cell system, which, in the case of a hybrid design, may also include an energy storage device (e.g., a battery and/or ultracapacitor), and associated control functions. The input to this block is the electric current drawn by the motor. The output is the voltage provided by the FC System to the dc terminals of the power electronics for the electric motor. For the case of a non-hybrid fuel cell vehicle this is the same voltage as the fuel cell stack voltage. In hybrid designs this voltage may be the battery voltage, or any other voltage, depending on the exact design and particularly depending on the location of the dc–dc converter that is normally used in hybrid designs.

The overall design of *FCVSim* incorporates two major feedback loops that simulate the physical dependence of the maximum motor torque of the electric drive train on the voltage supply and the motor speed (see Fig. 2). The physical origins of these feedback effects are:

- Mechanical feedback: As soon as the driver signals a torque request the electric drive train starts providing torque to the wheels. Because of this torque supply the vehicle accelerates and the motor speed increases. This increase in motor speed feeds back to the Drive Train block, to account for the sensitivity of the maximum motor torque to changes in motor speed.
- Electrical Feedback: As soon as the motor starts spinning it provides mechanical power to the wheels. It can only do this by drawing electrical power from the FC System block. As a result the motor draws an electric current from the fuel cell system. In general, the voltage generated by the FC System, and provided to the dc terminals of the power electronics, decreases as the load current increases. To account for the sensitivity of the maximum motor torque on the supply voltage, this decreased voltage is fed back to the electric drive train as a dynamic input.

The voltage decrease effect associated with the electrical feedback loop can be dramatic for a fuel cell power system, depending on the exact state of operation of the air and fuel supply variables relative to the power demand. Accounting for this effect is a critical requirement in providing a realistic dynamic simulation of any fuel cell vehicle.

These two feedback effects, together with the physical component characteristics, determine the overall dynamic characteristics of the combined drive train, power source and vehicle, which comprise the overall vehicle model. The setup of *FCVSim* is analogous to the physical setup of a real vehicle. The only physical interface between the drive train and the source of electric power is the electric connection between both components (excepting information flow for control purposes and the cooling system). This interface can be fully described by change of voltage and current versus time. On the mechanical side the physical interface variables between the drive train and the vehicle are the wheel torque and the wheel speed. Similarly, this interface can be fully described by calculating both mechanical variables values versus time.

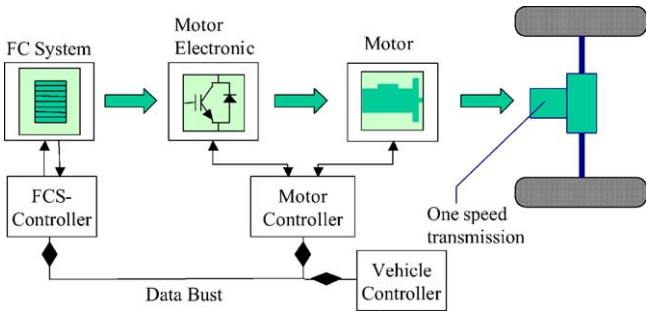

Fig. 3. Configuration of a generic FCV.

Fig. 3 shows the energy flow and arrangement of the main vehicle components in a generic fuel cell vehicle.

As shown in Fig. 3, the electric energy provided by the fuel cell system is fed into the electric drive train. The motor electronics converts the dc power at the fuel cell stack terminals into ac power fed to the terminals of the ac induction motor. The motor provides the mechanical shaft energy via a one-stage reduction gear and a differential to the wheels. A fuel cell controller, a motor controller and an overall vehicle controller contain control algorithms designed to provide optimum component interaction for all vehicle and component states.

To ensure that each of the components in the model is realistically represented, *FCVSim* incorporates either fundamental models (as in the fuel cell stack) or performance based maps (as in the electric motor and compressor). Some of the subsystems are separately modeled in greater detail, but frequently a simplified ("reduced") version of these subsystem models is then utilized within the vehicle level simulation, where appropriate for the simulation objective and to reduce simulation run time. This is done to ensure that the vehicle model will fully capture all the important characteristics of each component without unduly sacrificing simulation run time.

With the exception of the "FC System" block, detailed derivations and descriptions of each of the other *FCVSim* blocks are in the literature (Hauer [1], Hauer and Moore [2,4]).

3. Overview of *DH-FCVSim* model

This section provides an overview of the load-following direct-hydrogen fuel cell vehicle (DH-FCV) model that is the focus of this paper. In this paper the DH-FCV simulation tool is referred to as *DH-FCVSim*. It was developed to simulate a realistic dynamic DH fuel cell system and fuel cell vehicle.

DH-FCVSim simulates a direct-hydrogen vehicle configured as a load-following vehicle (without additional energy storage and without the provision of regenerative braking). Although *FCVSim*-based simulation tools have also been de-

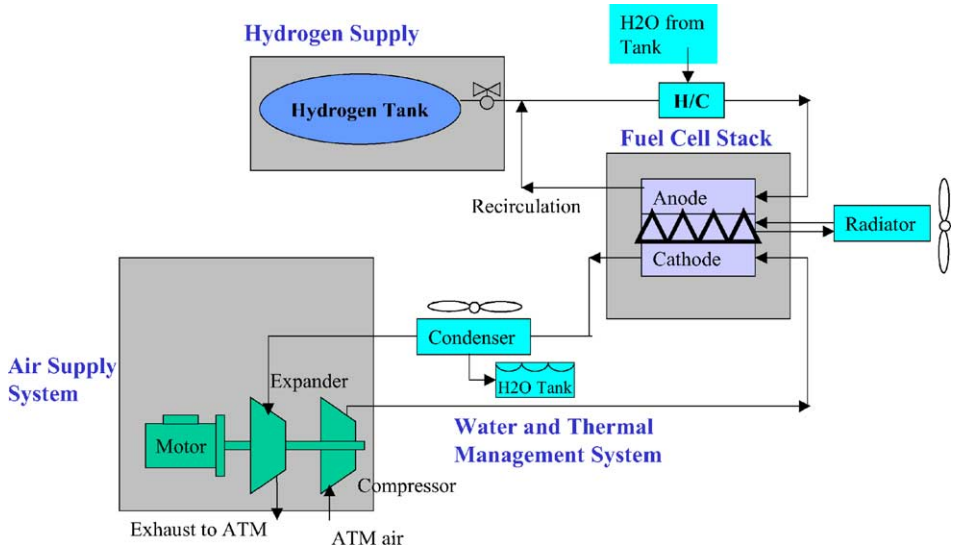

Fig. 4. DH fuel cell system diagram.

veloped for several hybrid versions of a direct-hydrogen FCV, these versions of the *FCVSim* tool are not discussed in this paper.

A controls engineering view of the direct-hydrogen fuel cells system is provided in Hauer and Moore [4]. The next portion of this paper focuses on the less abstract physical description of the direct-hydrogen fuel cell system implemented in the *DH-FCVSim* tool. For modularity reasons and to ensure proper comparisons among vehicle types all other aspects of the *DH-FCVSim* simulation tool are common to the general *FCVSim* tool. Fig. 4 illustrates the physical configuration of the DH Fuel Cell System simulated in *DH-FCVSim*.

There are four major subsystems illustrated in Fig. 4. They are:

- Fuel cell stack,
- Air supply system,
- Water and thermal management system,
- Hydrogen supply.

In the following sections of this paper, each of these four major subsystems of the DH fuel cell system is described, components and controls are discussed, and the specific simulation methodology is described and illustrated.

4. Fuel cell stack

The fuel cell stack provides the hydrogen energy conversion and is the power producer in *DH-FCVSim*. The "size" of the fuel cell stack is defined by the total number of cells together with the active area of each (nominally identical) cell. A simple block diagram of the fuel cell stack is given in Fig. 5.

In a DH fuel cell system the anode side of the fuel cell stack is supplied with pure hydrogen. The cathode side is supplied with oxygen from the ambient air by an air supply system (typically a compressor or a blower). The stack performance is strongly dependent on the anode and cathode conditions—pressure, stoichiometry and humidity, respectively.

The effect on cell/stack performance from changes in these variables will be illustrated in the following sub-sections. It cannot be overemphasized how important it is to both understand the shape of the fuel cell polarity plot and to realistically simulate its dynamic dependence on anode and cathode supply conditions, and electric power demand, quantitatively. This quantitative and dynamic dependence has a critical impact on FCV performance. This impact occurs through the voltage feedback effect illustrated in Fig. 2 and is due to the dependence of the available motor torque on the supply voltage at the terminals of the power electronics (as discussed earlier in connection with that figure). As the current (power) demanded from the fuel cell stack is increased the stack voltage decreases and this voltage decrease must be dynamically simulated to provide a realistic representation of FCV and fuel cell system performance.

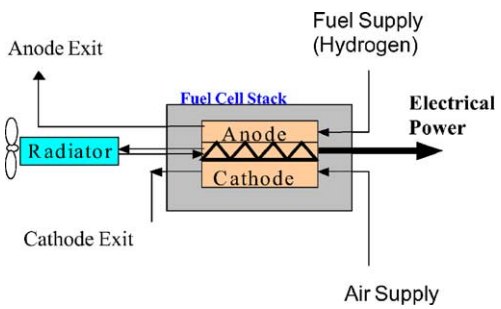

Fig. 5. Fuel cell stack.

4.1. Fuel cell and stack simulation description

The fuel cell simulation is based on a basic diagnostic fuel cell model derived and validated by Springer at Los Alamos National Labs (Springer et al. [6]). Using this basic cell model, a stack simulation model was developed to predict the stack voltage for varying stack current and varying anode and cathode conditions (pressure and mass flow rates). For an explanation of the detailed cell and stack model the reader is referred to the literature (Springer et al. [6], Friedman et al. [7]).

The following major effects are taken into account in the cell level simulation:

- Anode overpotential—reaction and transport losses in the anode catalyst layer,
- Concentration losses from diffusion in the anode backing layer,
- Cathode overpotential—reaction and transport losses in the cathode catalyst layer,
- Concentration losses from diffusion in the cathode backing layer,
- Ionic membrane resistance,
- Water management in the membrane,
- Electronic resistance of the catalyst layers.

In the simulation of the stack three Cell-level loss mechanisms are considered. These are:

- The cumulative Cell-level losses due to: the mass transport limitations and reaction losses on each of the cell anodes,
- The ohmic membrane losses for each cell,
- The cumulative Cell-level cathode losses due to mass transport and reaction losses on each of the cell cathodes.

4.2. Example results for Cell-level simulation

For the anode, the impact of the fuel supply is accounted for as a voltage loss that is a function of hydrogen mass flow rate, pressure, and current. Each particular mass flow rate, pressure, and current results in a different average partial pressure of hydrogen at the anode catalyst layer surface, and is associated with a different anode voltage loss.

The ohmic membrane loss is due to the ionic resistance of the membrane plus both catalyst layers, and the electronic and contact resistance in the catalyst layer, the backing layer and the bipolar plates. This loss is modeled as proportional to the applied stack current.

On the cathode side the impact of air supply is accounted for as a voltage loss that is a function of the average partial pressure of oxygen at the catalyst layer-gas diffusion layer interface and the stack current. As with the anode, each particular mass flow rate, pressure, and current results in a different average partial pressure of oxygen at the cathode catalyst layer surface and is associated with a different cathode voltage loss.

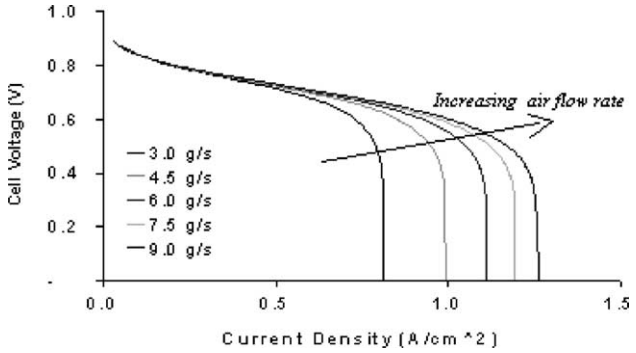

Fig. 6. Simulation of fuel cell voltages for variation in airflow rate.

Fig. 6 shows the results of the cell simulation for the variation in cell voltage and current density due to different air mass flow rates at constant pressure. The primary impact is the strong limitation in maximum current density for each mass flow rate, with a relatively smaller effect on cell voltage (except near the limiting current value).

Fig. 7 illustrates the simulation at the cell level when the air pressure is varied with no change in the mass flow rate of the air. In this case, a substantial voltage variation is generated for all current densities, but there is only a minor impact on the maximum current density value.

Fig. 8 illustrates a set of "optimized" cell polarization curves for the DH case—with curves for indirect methanol (IM) and indirect hydrocarbon (IH) stacks shown for contrast (The lower voltages for the IM and IH stacks are primarily due to the hydrogen dilution in the reformate fuel streams.). The anode conditions are not constant for this figure and the individual anode conditions are listed inside the plot.

The cathode conditions that are employed to generate these "optimum" curves are the result of a system efficiency optimization process that takes into account the stack, air supply, and the water and thermal management (WTM) requirements at each current density demand. The optimization process is discussed in Section 5. Note that in general, because of transient effects discussed later, these optimum results are not achieved throughout an entire dynamic drive cycle.

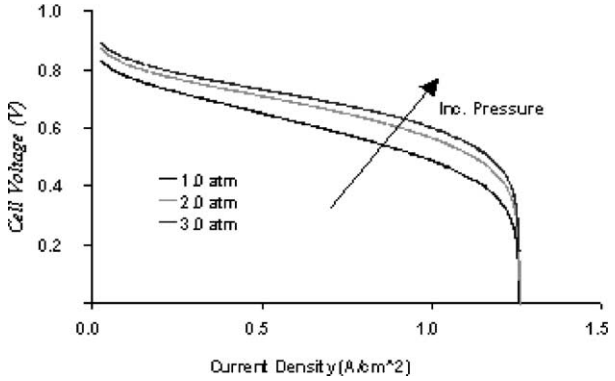

Fig. 7. Simulation of fuel cell voltages for variation in air pressure.

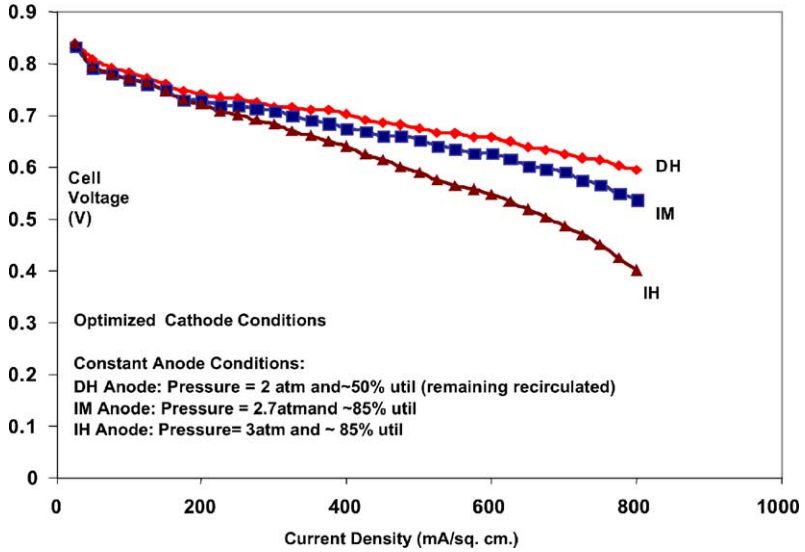

Fig. 8. "Optimized" polarization curves for the DH, IM, and IH fuel cells.

The "optimized" curves in Fig. 8 depend upon the exact characteristics of the specific air supply system and the WTM control and components used in a particular fuel cell system. The curves shown here (for a particular choice of stack, air supply, and WTM components) are purely illustrative, and therefore must not be interpreted quantitatively as general results.

Because of the close link between the air system and the stack sizing in developing the optimum air supply-stack control strategy, the *DH-FCVSim* user is only able to select specific stack and air system combinations (rather than individual components) in the simulation. This issue is discussed in detail in Section 5.

4.3. Stack simulation implementation

The key assumptions for the Stack simulation are:

- Adequate water management is provided such that cell resistance remains constant with current and no water flooding effects are seen in the cathode.
- All cell voltages are equal for a given stack current. The number of cells and the area of each cell are specific to each Stack.

At its top most level, the fuel cell stack model takes the inputs of hydrogen utilization, hydrogen concentration, current demand, air stoichiometric ratio, and air pressure to calculate

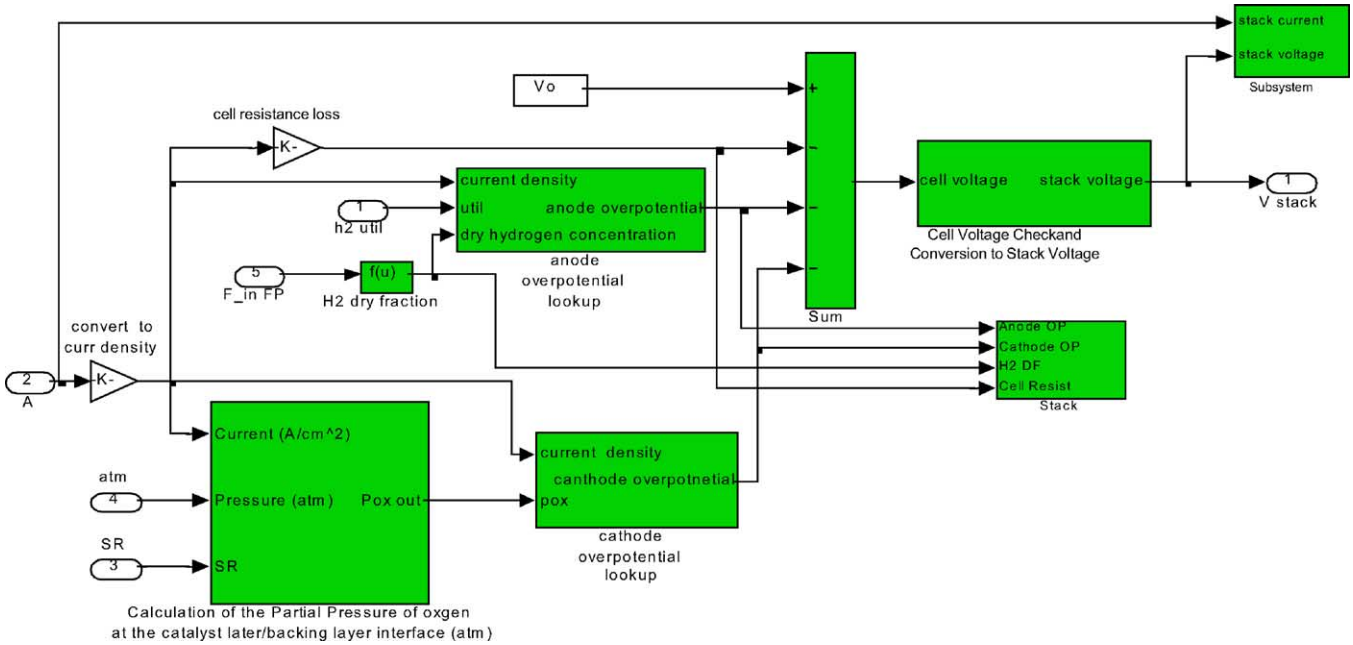

Fig. 9. Details of the Simulink fuel cell stack block.

the cell and stack output voltage under each specific set of dynamically varying operating conditions. The purpose of the calculation is to dynamically simulate the voltage–current characteristics of a fuel cell stack operating on pure hydrogen and air within an FCV. The Simulink block that carries out this calculation within the DH fuel cell system simulation is shown in Fig. 9.

As illustrated in Fig. 9, the Simulink fuel cell stack block includes the lower level blocks that calculate and sum up the various losses associated with stack operation at the conditions determined by the dynamic input variables—hydrogen utilization, hydrogen concentration, current demand, air stoichiometric ratio, and air pressure. The details of this stack simulation process is further discussed in the literature (Friedman et al. [7,8]).

5. Air supply

The DH fuel cell system utilizes an air supply subsystem with an associated control scheme. The air supply can be operated either at high pressure (using a compressor) or at low pressure (using a blower). Both designs have been demonstrated for automotive applications. A comparison of these two modes of operation is available in the literature (Cunningham et al. [9]).

Fig. 10 shows the components for a high-pressure cathode air loop that is simulated in *DH-FCVSim*. The control scheme developed to maximize the system efficiency at each system power level is discussed later. An "atmospheric" pressure air supply using a blower is also available for simulation in *DH-FCVSim*.

The illustrated air supply includes a compressor with a variable speed electric motor. The compressor drives the pressure and mass flow of the cathode air loop, although other components play important roles in the overall operation of the airflow loop. Compressed air is sent directly into the cathode of the fuel cell stack where oxygen is depleted for power generation. A condenser component is included in the cathode exhaust path to recover liquid water (for recirculation into the anode fuel loop, as required), but no humidifier is included for control of the air humidity entering the cathode.

In addition to the interaction with the fuel cell stack, the air system also interacts with WTM components and impacts the WTM control strategy. Following the stack reactions, it is necessary to recover liquid water from the stack exhaust stream—primarily for recirculation into the anode fuel loop of the DH system. This exhaust stream consists of excess oxygen, the unused nitrogen, and water liquid and vapor. If the amount of liquid water is not sufficient for system water requirements, a condenser is necessary to recover additional liquid water from the vapor phase. The WTM operation and control strategy is discussed separately in a later section.

In the following subsections the compressor air supply simulation model is first discussed in more detail, the air supply control optimization scheme is then introduced, transient effects are brought into consideration, and finally the implementation of the compressor air supply model within Simulink is described.

5.1. Description of the air supply model

The complete requirements for a flexible and realistic air supply simulation in an FCV model are described in detail in the literature (Cunningham et al. [11]). The compressor air supply system used in *DH-FCVSim* is described briefly below.

Multiple compressor technologies are available, and one blower technology is available, for comparison modeling among air supply technologies. They include the following:

1. Twinscrew compressor (with 2.45 PR max),
2. Piston compressor (second generation, designed for fuel cell applications),
3. Centrifugal compressor (designed for fuel cell applications),
4. Regenerative blower.

The air supply model is able to use an expander combined with the three compressor options listed above.

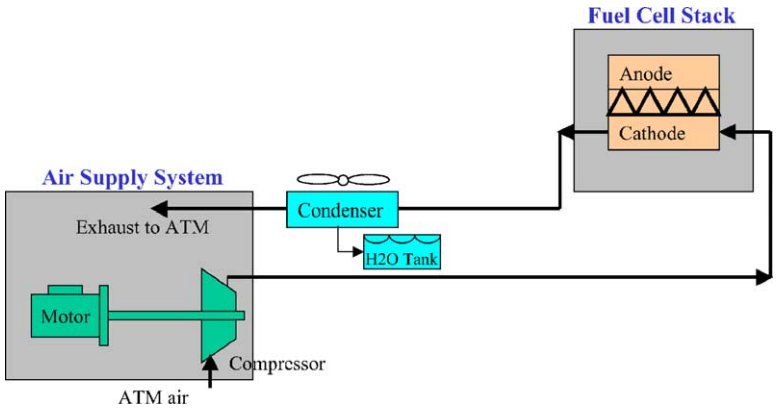

Fig. 10. High-pressure air supply in the fuel cell system.

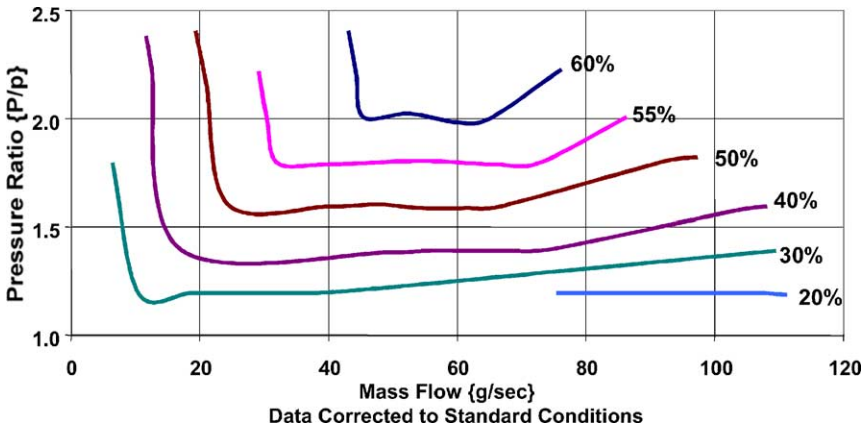

Fig. 11. Twinscrew compressor efficiency.

For the examples in this paper, a twinscrew, positive displacement compressor (number 1 from list above) is chosen. It has a maximum pressure ratio (PR) capability of 2.5 and a maximum air mass flow rate of 105 g/s at a maximum pressure ratio of 1.8 (assuming STP conditions). Fig. 11 illustrates the experimental performance of the twinscrew compressor incorporated into the model. This data is used to determine the air compressor parasitic load.

The experimental efficiency values plotted in this figure incorporate the mechanical losses in the compressor device as well as the isentropic efficiency of compression. Therefore, the efficiency is expressed at the shaft of the motor. The shaft mechanical input power for each particular set of operating conditions (pressure ratio and mass flow) of the compressor can be calculated from the information in this figure.

Additionally, a variable speed motor and controller map is utilized to determine the input electric power (auxiliary load of the air supply) required to provide a given compressor shaft speed and torque. The motor operates with a current draw from the fuel cell stack at the voltage produced at the stack. Control of the backpressure applied to the compressor, and control of the motor shaft speed, allow for the delivery of the desired airflow into the fuel cell stack.

5.2. Air supply control optimization

One unique feature of the *DH-FCVSim* model is the optimization process that includes the effects of stack, air supply, and WTM on system efficiency. A separate stand-alone steady-state "optimization" model is used to determine the combination of air supply, stack, and water/thermal management performance that maximizes the steady-state system efficiency over the net electrical power range. This provides a control target for the operation of these components. This process accounts for the fuel cell stack performance, the parasitic load of the air supply, and the parasitic loads of the condenser and radiator for the WTM system in determining the optimum air supply control strategy. The results of this optimization are used in the control strategy for the air loop operation under dynamic power demand. This steady-state optimization process is outlined below, and a detailed description of the process is available in the literature (Friedman et al. [7], Friedman et al. [10]).

The gross power of the fuel cell stack is directly dependent on the average partial pressure of oxygen at the cathode catalyst reaction sites. Each single value of average partial pressure of oxygen corresponds to a particular cell voltage value at a particular current density, and is a function of both the total air pressure and the air mass flow rate. For this reason, a compressor that can provide variable flow and pressure is required to provide a broad range of stack power operation with minimum energy consumption (high efficiency) for the high-pressure air supply system.

The (net) electric system power is simply the stack (gross) electric power minus the parasitic loads of the air system electric motor (calculated from the air system model used for the optimization process) and the WTM radiator and condenser loads.

Different pressure and air mass flow combinations lead to different water states (vapor percent versus liquid percent) in the fuel cell cathode exhaust. Both of these factors have ramifications on condenser and radiator loads and will affect parasitic (pump and fan) electric demands. For this reason, the condenser and radiator loads are taken into consideration when determining the optimum air system control strategy.

The control strategy derived from the optimization process represents an optimized simulated steady-state operation. In other words, for each net electric power value demanded of the fuel cell system the optimization model provides a "target" air pressure and mass flow rate at which to operate the system in order to maximize steady-state system efficiency at that net power level. However, this target will not generally be achieved for every instant during actual model simulation of a drive cycle, because of transient limitations in the air supply system.

Example results from this steady-state optimization – for the twinscrew compressor technology used for illustration here – are summarized in Fig. 12. This figure shows the

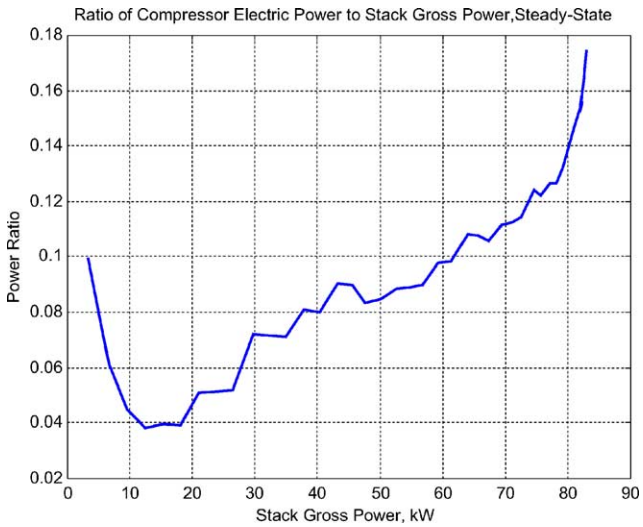

Fig. 12. Air supply power ratio vs. stack power.

"optimized" ratio of the compressor electric power loss to the gross power from the fuel cell stack—plotted for the complete range of the stack's gross power capability. This is the ratio for optimized steady-state operation at each power level (i.e., using the optimum variable pressure and mass air flow at each point) and is not generally achieved during very dynamic system operation. These are the operating points that the control system seeks within the limitations of transient response.

For this compressor technology, operated in an optimum steady state at each power level, Fig. 12 shows that the power required for the compressor can be quite small (<10% relative to the stack gross power) in the partial load regions (10–60% of peak stack power). However, near full power operation this compressor is forced to operate in a less efficient region of performance to provide the required air mass flow, and the relative power ratio begins to increase (approaching 20% of stack gross power).

Also there is a sharp increase in the power ratio at very low stack power. This increase in the power ratio at the very low power region occurs because the compressor has a minimum (idle) air flow that it must provide (technology limited)—this flow must be provided regardless of the actual stack air requirements or stack output power needed for other auxiliary loads.

Over the range of system net power load, the pressure and airflow demands vary with the power demand value. The air mass flow steadily increases from the minimum (idle) airflow up to the peak airflow value as the power demand increases. The pressure, however, does not necessarily exhibit a simple monotonically increasing characteristic. The exact shape of the optimum pressure curve versus system power depends on the detailed performance of the compressor technology. For example, although the pressure is higher at peak power than at minimum power, the optimized pressure line for the specific twinscrew compressor technology illustrated here occasionally decreases for increases in electric power demand.

The air supply subsystem cannot respond instantaneously. In general, there are two primary system characteristics that result in a transient delay in air supply to the cathode. That is, between the time when the compressor motor is supplied with sufficient electrical power (relative to a demanded air pressure and air mass flow) until the time that the desired air pressure and flow reach the fuel cell stack cathode reaction sites. First, there is a time associated with changing the state of the air in the entire physical volume of pipes and cathode channels. This may be thought of as "charging" the complete air flow system. The time delay will be relatively larger, for example, if the system needs to be changed from a low pressure (i.e., 1.2 atms) to a higher pressure (i.e., 3 atms). The second time delay is associated with the inertia of the compressor shaft movement.

To account for the combination of these effects, the simulation of the air supply system includes a time delay feature that retards the supply of air pressure and air mass flow relative to the demanded stack current. This delay introduces a transient into the air supply fuel cell system response to a change in vehicle power demand (accelerator position), and causes a lag in the power provided by the fuel cell system—as well as leading to air system operation off the optimum efficiency point for the demanded power.

5.3. Simulation model implementation

The *DH-FCVSim* model user has a Graphical User Interface (GUI) specifically for the optimized air system plus fuel cell stack. With this interface, the user can choose from several optimized stack-compressor files. Performance characteristics can be viewed in the GUI. Output results include compressor and stack air conditions throughout the vehicle simulation. Fig. 13 is the Simulink implementation of the air supply.

Operation of this block is initiated by the input of total stack current required by the fuel cell system, a surrogate for system power demand. This input enters the "compressor control scheme block" where it is used to determine the required stack operating PR and air mass flow rate (mdot). This is accomplished with map information originally calculated in the optimization model (where the stack pressure ratio and air mass flow are optimized as a function of current).

Following the "control scheme block", air system characteristics related to the fuel cell stack are calculated. The pressure drop along the cathode channels in the stack is accounted for and summed with the stack pressure to determine the demanded PR at the compressor. Additionally, the SR associated with the operating mass flow and total stack current is calculated and used as an input to the "fuel cell stack block" (not shown in this figure).

Finally, the compressor/expander shaft and electrical characteristics for the demanded PR and mass flow are calculated. Shaft power and speed are determined using map information from air system developers. Recovered shaft power from the use of an expander is included, if utilized. The net shaft power

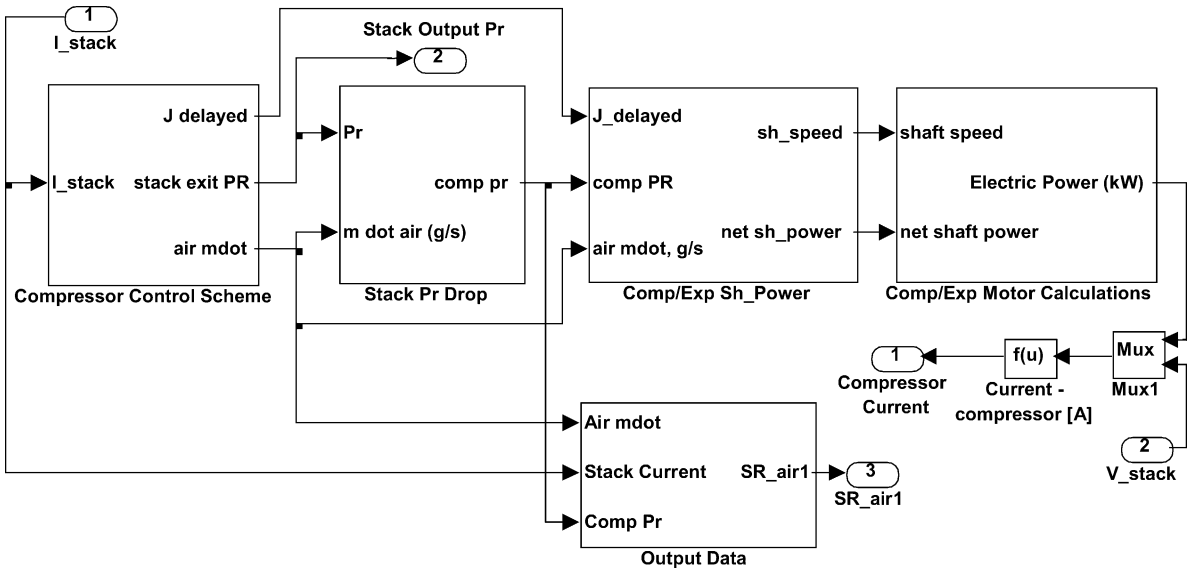

Fig. 13. Detail of the Simulink air supply model.

and speed is then used to calculate shaft torque followed by the associated electrical power needed at the motor terminals. The last step is to utilize the electrical power and the stack voltage and calculate the necessary electrical current needed to operate the compressor. This becomes an output and is used in the fuel cell system control scheme.

An expander (turbine) simulation is provided within the *DH-FCVSim* model structure. This allows the model to account for recovered shaft energy with the use of an expander. Output shaft power from this device is included in the vehicle model as a look-up table. The key assumptions are:

- The stack gross power is calculated using the stack exit air pressure conditions.
- The air system model utilizes one motor map scaled for the different technologies.
- "Turbo-lag" between the compressor and the expander is not considered.

A detailed discussion of the implications and requirements for including an expander in the air system is available in the literature (Cunningham et al. [12]).

6. Water and thermal management

This section briefly describes the basic elements of a water and thermal management subsystem, WTM system, for a DH fuel cell vehicle. Detailed descriptions are available in the literature (Badrinarayanan et al. [13,14]).

The discussion of the fuel cell system and components in this section is from a WTM viewpoint. In other words, the component descriptions are greatly simplified to focus on only the aspects that affect the WTM subsystem operation.

The WTM system diagram is illustrated (within the fuel cell system context) in Fig. 14.

The WTM subsystem refers to the primary heat transfer component (radiator) and primary water recovery unit (condenser) within the fuel cell system. In the WTM model these two components are analyzed in the context of the fuel cell system to determine their impact as a parasitic power loss for the system. The process of WTM calculation, optimization, and control considers all other components in the system, but only in the context of heat and water balance. For example, from the perspective of the WTM, the fuel cell stack is viewed only as a heat source, a water production component, and a heat storage device.

The vehicle radiator has the primary function of maintaining the fuel cell stack at its operating temperature. As discussed below, the heat load is given by the combination of the stack heat rejection due to inefficiency and due to water condensation in the stack. Even though the fuel cell stack is substantially more efficient as an energy converter than an

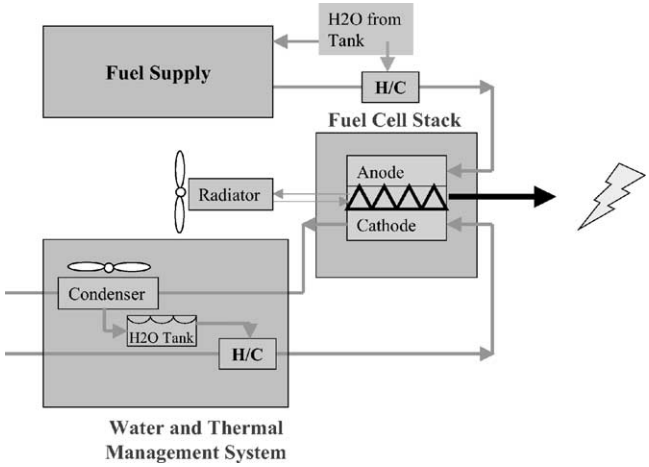

Fig. 14. WTM system diagram.

internal combustion (IC) engine, the amount of heat that has to be dissipated through the fuel cell system cooling circuit is much larger. This is because relatively little heat is carried away in the exhaust of the fuel cell (<10%) as opposed to the energy content of the high temperature exhaust of the IC engine (>33%). Additionally, because the stack generally has a narrow window of optimal temperature operation, the required flow rates of coolant through the radiator can be substantial for high power operation of the stack.

The condenser in the DH system is placed in the cathode exhaust stream and provides any additional liquid water that is needed by the system (in the DH system this is used for injection into the anode fuel stream).

6.1. Heat balance within the DH fuel cell system

The stack generates heat by two primary mechanisms: (1) the inefficient conversion of hydrogen chemical energy into electrical energy, and (2) the condensation of water inside the stack. The combination of these two heat sources determines the thermal load on the radiator.

The amount of heat due to losses in the stack conversion process for the hydrogen chemical energy is directly related to the stack efficiency. The stack efficiency is calculated in the simulation as the gross electrical power produced by the stack divided by the lower heating value of the fuel (H_2) used in the stack. It is important to note that the stack efficiency is based on the fuel used within the stack as opposed to the fuel supplied to the stack (some of which is not consumed and is recirculated in the anode loop). The lower heating value is used for this calculation to represent the case where all of the water exits in the stack in vapor form. This is not always the case and the value is later corrected for the fraction of water condensed within the stack, as discussed below.

Because of the substantial heat generation by the stack, and the small temperature differential between the coolant and ambient temperature, fuel cell vehicles can require large radiators. The radiator simulation is based on a lookup table that uses empirical data generated from a modern standard brazed aluminum, single-pass radiator with 33 tubes (Ricardo [17]) under the assumptions of:

- No ram-air effect (all air flow due to radiator fan). Including ram-air will reduce the load on the condenser fan.
- Temperature difference of coolant maintained at 5 °C. Will require variable flow rate coolant pump (not modeled here).
- Constant fan efficiency of 50%. This is a conservative assumption. A real fan would have an efficiency map based on torque and speed.

In a vehicle system, it is likely that the radiator fan will be sized for a specific peak load. This is generally thought of in terms of continuous peak power or grade-ability. This peak power is frequently not the maximum power the system can produce. Therefore there will be situations when the radiator is not able to remove all the heat that the stack produces. When this occurs, the stack acts like a thermal storage medium. The rate at which the stack stores heat is a function of the weight of the stack and the specific heat of the stack, and the rate at which the temperature of the stack rises when all the heat cannot be removed by the coolant. Additionally, when the stack is above it's operating temperature and operating below the maximum heat removal of the coolant, the time required to cool the stack back down to the operating temperature can be calculated under the assumption that all heat loss is through the coolant loop.

6.2. Water balance within the DH fuel cell system

Efficient operation and durability for a PEM fuel cell stack requires that each cell membrane, and catalyst layers, be very well hydrated. If water is not continuously provided to the anode, the lack of proper hydration can cause significant increases in cell resistance and the overpotential of the cell anode reaction. Various methods are practiced to provide this anode water input. A common approach is to continuously humidify the anode stream (with water recovered from the cathode exhaust stream). In this model, the water input to the anode is simulated as direct water injection into the air stream as it enters the anode plenum.

For the DH fuel cell system considered here, water is injected into the anode fuel stream to produce 100% relative humidity (RH) at the fuel cell stack operating temperature prior to entry into the stack. Therefore, because of recirculation of the anode stream (i.e., no exhaust to ambient), the net water injection requirement for the anode is equal to the water dragged from the anode to the cathode (electro-osmotic drag effect). This water drag value is dependent on the stack current and the state of hydration as a function of distance through the membrane. For the *DH-FCVSim* model it is calculated from a separate detailed stack model (Badrinarayanan et al. [14]).

There is disagreement in the literature on whether humidification of the input cathode air stream is necessary to insure good fuel cell stack performance. Some authors claim that it improves membrane humidification and thermal management of the air supply (Pischinger et al. [15]), while others indicate that it is not necessary in a well designed system and may even make water and thermal management more difficult (Wilson et al. [16]). The model allows either choice to be made in a simulation.

All of the water required for the fuel cell system is condensed at the exhaust of the stack cathode. The cathode exhaust consists of nitrogen, residual oxygen, and water. The water in the cathode exhaust can be from four different sources:

- Water production at the cathode due to the cathode reaction.
- Net water dragged from the anode to the cathode by proton flow.

- Ambient humidity in the inlet cathode air stream.
- Water injected for cathode inlet air humidification.

The water in the stack cathode exhaust can exit as either vapor or liquid form, and, most commonly, is a two-phase mixture. The amount of water that condenses within the stack is a strong function of the cathode operating parameters of air pressure and air mass flow rate. For the water that exits in liquid form, the amount of heat rejected by condensation has to be accounted for in the calculation of the stack heat generated (because the calculation of the hydrogen conversion heat generation in the stack used the lower heating value for hydrogen).

The WTM simulation calculates the water required for the system. Given the cathode conditions some amount of that water may have already condensed within the stack and is available in the liquid phase. The condenser is then operated to condense any additional liquid water needed to meet the system requirement.

The major assumptions used in the condenser simulation are:

- All water is condensed at cathode exhaust (no anode exhaust condenser). While this is not an issue for the DH system (because of hydrogen recirculation), IM and IH fuel cell systems can lose significant water through the anode exhaust.
- There is no ram-air effect (i.e., all airflow is due to the condenser fan). This is conservative case, since including ram-air will reduce the load on the condenser fan.
- A constant fan efficiency of 50%. This is a conservative assumption. A real fan would have an efficiency map based on torque and speed.

The model of the air–air condenser that is used for this purpose is based on a cross flow heat exchanger.

6.3. Optimized operation of WTM subsystem

In general, the parasitic loads of the WTM system are small in comparison with the other auxiliaries of the fuel cell system (air supply, fuel processors, etc.) for a well designed fuel cell system with optimized WTM control. It is important to note that this is for an optimized system (one in which the WTM and air supply loads are minimized in comparison to the stack output at each operating point) and for one with the relatively large heat-transfer areas used in this model. Other design choices can be made that will increase the WTM parasitic loads significantly.

The WTM system is included in the overall optimization of the cathode (air) side operating strategy for the compressor. Because the WTM system is strongly affected by the air pressure and flow rate (stoichiometry), its optimization impacts the air supply optimization scheme.

The optimization process used here for the fuel cell system can be thought of as maximizing the net power of the system at each operating point based on controllable operating parameters. The WTM loads are dependant on the system operating parameters (cathode pressure and cathode stoichiometry) and it is important to include WTM loads while performing an overall system optimization. The objective of the optimal operating scheme (on the cathode side) is to determine a pressure ratio and mass flow rate that maximizes the net steady-state power from the fuel cell system at every operating point. The full optimization procedure is described in detail in the literature (Friedman et al. [10]).

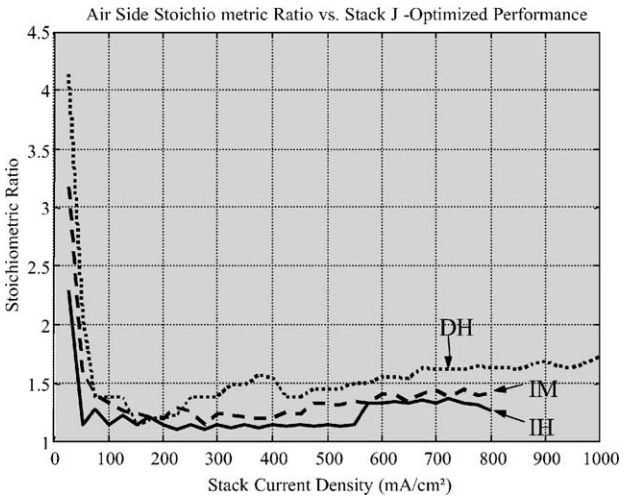

Fig. 15. Optimized cathode stoichiometric ratio.

Examples of the resulting optimization curves for the air-side operating parameters are shown in Figs. 15 and 16. The curves for the DH system are compared with optimization results for the IM and IH systems. Both the IM and IH fuel cell systems have substantially higher system water requirements, essentially because of the fuel processor water and air requirements in these systems.

It is also important to note that the optimal air pressure and stoichiometry for each stack operating point is strongly influenced by the size and design of the WTM and air supply components. Increasing or decreasing the size or heat transfer

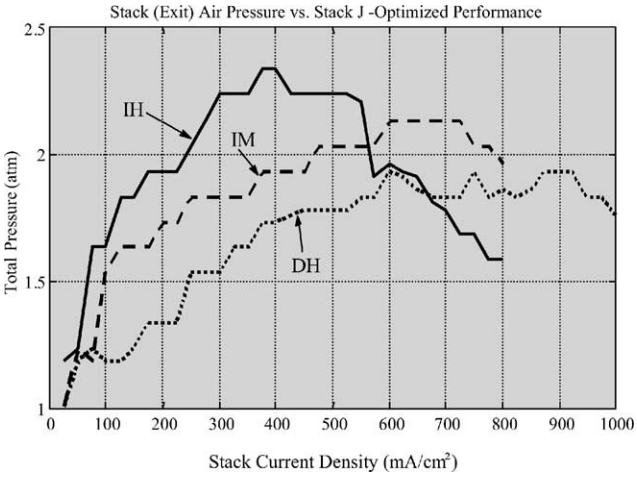

Fig. 16. Optimized cathode pressure ratio.

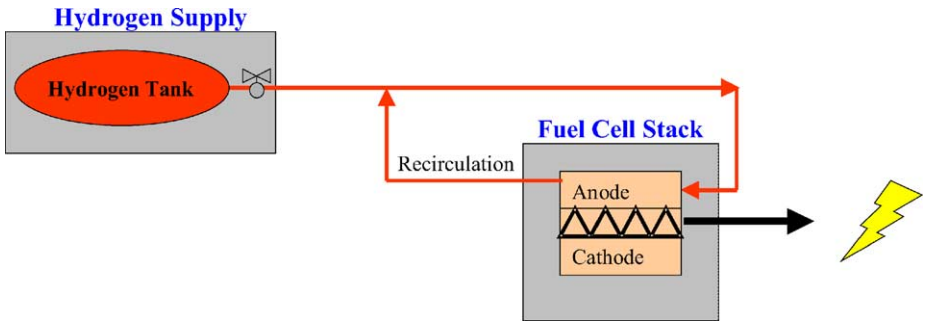

Fig. 17. The hydrogen supply system in the fuel cell engine.

coefficient of the radiator or condenser, as well as changing the air supply (compressor, blower, expander, etc.) can significantly shift the optimal operating points. In this way, the optimal sizing of the system is part of the overall optimization process. The optimal sizing of components is a design issue that is not discussed here, but is critical to achieving low values of air supply losses and WTM losses for the fuel cell system.

6.4. Implementation of model

The WTM model uses the instantaneous system current, stack voltage, air supply stoichiometric ratio (SR), and air supply PR as inputs, and calculates as an output the auxiliary load of the WTM system (in terms of the current required at the fuel cell stack output voltage). In addition, other outputs available from this model for analysis purposes are the instantaneous water recovered, instantaneous water requirement, cumulative water availability, stack temperature, radiator load, condenser load, and total WTM auxiliary load as a function of time throughout the simulation.

In effect, the WTM model calculates the total power required by the condenser and radiator system to try to control system thermal and water balance on an instantaneous basis. Dividing this power requirement by the stack voltage, the WTM model then calculates a current that represents the load of the WTM system as an additional current that must be provided by the fuel cell system (an increased fuel and air flow requirement and different operating point). This parasitic power requirement is included as a system loss in the calculation of the DH fuel cell system efficiency.

7. Hydrogen supply

The goal of the hydrogen supply modeling process is to determine the hydrogen storage and delivery characteristics that may affect the system performance, and to feed this information into the system model.

The hydrogen supply subsystem is illustrated in Fig. 17. It basically consists of a high-pressure (5000 psi) hydrogen tank for the hydrogen storage, and a recirculation loop to add the unused hydrogen in the stack exhaust into the flow of fresh hydrogen from the storage tank. An ejector pump is assumed to provide the recirculation for the hydrogen from the anode exhaust.

In comparison with the potential time delays associated with the air supply, or the fuel processor systems required for indirect methanol and indirect hydrocarbon fuel cell systems, no significant dynamic effects exist for the hydrogen supply system. Therefore, it is assumed that there is negligible time delay in providing the requested hydrogen flow from the storage tanks at the required pressure, and no time delay is included in the hydrogen supply subsystem model. Thus, the compressed hydrogen supply plays no role in the dynamic response of the fuel cell system.

Since an ejector pump (using the Venturi effect) provides recirculation of the hydrogen, it is assumed that there is no parasitic power required for the recirculation of the exhaust hydrogen. Therefore, the hydrogen supply also plays no role in the optimization of the fuel cell system operation and has no effect on the fuel cell system energy conversion efficiency.

The hydrogen tank size is modeled to provide information on the physical volume needed for storage, and to compute the tank's mass so that this can be include in the total vehicle mass for vehicle dynamics simulation.

Output information from the hydrogen supply simulation includes the tank pressure and the mass of hydrogen in the tank at any given time during the simulation.

8. Summary

This paper introduces and describes the load-following DH version of the general *FCVSim* fuel cell vehicle simulation tool. The emphasis is on the simulation of a Direct Hydrogen fuel cell system within the general *FCVSim* simulation tool, which was developed to provide a dynamic and realistic FCV simulation tool.

This specific DH fuel cell vehicle simulation tool presented in this paper is referred to as *DH-FCVSim*. *DH-FCVSim* simulates a direct-hydrogen vehicle configured as a load-following vehicle (without additional energy storage and without the provision of regenerative braking). Although *FCVSim*-based simulation tools have also been developed for a variety of other FCV designs, including hybrids, these

other tools are not discussed in this paper. Only brief descriptions of the vehicle subsystems in the general *FCVSim* vehicle model are provided as background, and this paper focuses on the subsystems that are specific to the load-following direct-hydrogen FCV model, *DH-FCVSim*.

There are four major subsystems that are specific to the load-following direct-hydrogen model, *DH-FCVSim*. They are: the fuel cell stack, the air supply, the water and thermal management system, and the hydrogen supply. In the major sections of this paper, each of these four major subsystems is described, components and controls are discussed, the specific simulation methodology is presented, and the general results available from the *DH-FCVSim* tool are illustrated by examples, where that appears useful and effective.

Acknowledgements

The research reported here was supported by funds provided by the members of an international consortium (DaimlerChrysler, Fiat, Ford, GM, Honda, Hyundai, Isuzu, Toyota, Nissan, Subaru, VW, BP, ChevronTexaco, ConocoPhillips, ExxonMobil, Petrobras, Schlumberger-Doll, Eaton, Regenesys, Ricardo, UTC, Xcellsis, the CaARB, and the USDoE). Further details and Publications of the Fuel Cell Vehicle Modeling Project are available at <http://fcv.ucdavis.edu>.

References

[1] K.H. Hauer, An Analysis Tool For Fuel Cell Vehicle Hardware and Software (Controls) with an Application to Fuel Economy Comparisons of Alternative System Designs, Dissertation, UC California, Davis, USA, 2001.

[2] K.H. Hauer, R.M. Moore, Fuel Cells for Automotive Applications, Professional Engineering Publishing, 2003 (pp. 157–177, ISBN 1860584233).

[3] K.H. Hauer, R.M. Moore, Fuel Cell Vehicle Simulation – Part 1: Benchmarking Available Fuel Cell Vehicle Simulation Tools, Fuel Cells – From Fundamentals to Systems 03/2003, Germany, 2003.

[4] K.H. Hauer, R.M. Moore, Fuel Cell Vehicle Simulation – Part 2: Methodology and Structure of a New Fuel Cell Simulation Tool, Fuel Cells – From Fundamentals to Systems 03/2003, Germany, 2003.

[5] K.H. Hauer, R.M. Moore, Fuel Cell Vehicle Simulation – Part 3: Modeling of Individual Components and Integration Into the Overall Vehicle Model, Fuel Cells – From Fundamentals to Systems 03/2003, Germany, 2003.

[6] T. Springer, T. Zawodzinski, S. Gottesfeld, Polymer electrolyte fuel cell model, J. Electrochem. Soc. 138 (8) (1991) 2334–2342.

[7] D.J. Friedman, R.M. Moore, PEM Fuel Cell System Optimization, in: Proceedings of the 2nd International Symposium on Proton Conducting Membrane Fuel Cells II, vol. 98/27, 1999, p. 407; Electrochem. Soc.

[8] D.J. Friedman, Reformate fuel cell stack characteristics and system interactions, in: 35th Intersociety Energy Conversion Engineering Conference, Las Vegas, NV, 24–28 July 2000 (paper number 2000–3045).

[9] J.M. Cunningham, M.A. Hoffman, D.J. Friedman, A comparison of high-pressure and low-pressure operation of PEM fuel cell systems, in: SAE 2001 World Conference, Detroit, MI, 5–8 March 2001 (paper number 2001-01-0538).

[10] D.J. Friedman, A.R. Eggert, P. Badrinarayanan, J.M. Cunningham, Balancing stack, air supply, and water/thermal management demands for an indirect methanol PEM fuel cell system, in: SAE 2001 World Conference, Detroit, MI, 5–8 March 2001 (paper number 2001-01-0535).

[11] J.M. Cunningham, M.A. Hoffman, R.M. Moore, D.J. Friedman, Requirements for flexible and realistic air supply model for incorporation into fuel cell vehicle (FCV) system simulation, in: SAE Future Transportation Technology Conference, Costa Mesa, CA, 17–19 August 1999 (SAE paper number 1999-01-2912).

[12] J.M. Cunningham, M.A. Hoffman, A.R. Eggert, D.J. Friedman, The implications of using an expander (turbine) in an air system of a PEM fuel cell engine, in: Proceedings of the 17th International Electric Vehicle Symposium & Exposition, Montreal, Canada, 15–18 October 2000.

[13] P. Badrinarayanan, A.R. Eggert, R.M. Moore, Minimizing the water and thermal management parasitic loads in fuel cell vehicles, Int. J. Transport Phenomena 3 (3) (2001).

[14] P. Badrinarayanan, S. Ramaswamy, A. Eggert, R.M. Moore, Fuel cell stack water and thermal management: impact of variable system power operation, in: SAE 2001 World Conference, Detroit, MI, 5–8 March 2001 (paper number 2001-01-0537).

[15] S. Pischinger, C. Schönfelder, W. Bornscheuer, H. Kindl, A. Wiartalla, Integrated Air Supply and Humidification Concepts for Fuel Cell Systems, SAE 2001-01-0233.

[16] M. Wilson, C. Zawodzinski, S. Gottesfeld, Direct liquid water hydration of fuel cell membranes, in: S. Gottesfeld, et al. (Eds.), Proceedings of the Second International Symposium on Proton Conducting Membrane Fuel Cells II, Electrochemical Society, Pennington, NJ, 1999.

[17] Ricardo Consulting Engineering LTD, Q vs. Air Mass Flow Curves for Modern Radiator, fax received on August 21, 2000.